

# Peritumoral Activated Hepatic Stellate Cells Predict Poor Clinical Outcome in Hepatocellular Carcinoma After Curative Resection

Min-Jie Ju, MD,\* Shuang-Jian Qiu, MD,\* Jia Fan, MD, Yong-Sheng Xiao, MD, Qiang Gao, MD, Jian Zhou, MD, Yi-Wei Li, MM, and Zhao-You Tang, MD

**Key Words:** Hepatocellular carcinoma; Peritumoral microenvironment; Hepatic stellate cells; Inflammation; Prognosis

DOI: 10.1309/AJCP86PPBNGOHNLL

## Abstract

*The inflammatory components of the liver remnant after hepatocellular carcinoma (HCC) resection are of prognostic importance. We evaluated prognostic potential of peritumoral activated hepatic stellate cells (HSCs) in 130 HCC cases. The messenger RNA (mRNA) levels of the functional genes in HSCs (ie, seprase, osteonectin, and tenascin-C), quantitated by real-time quantitative polymerase chain reaction, and the density of peritumoral Foxp3+ T-regulatory cells (Tregs) and CD68+ macrophages (MΦ), assessed immunohistochemically in tissue microarray sections, were positively correlated with the density of peritumoral activated HSCs. The density (P = .007 for recurrence-free survival [RFS] and P = .021 for overall survival [OS]) and functional genes (seprase, P = .001 for RFS; osteonectin, P = .007 for RFS and P = .021 for OS) of peritumoral activated HSCs independently contributed to high recurrence or death rates, as did peritumoral Tregs or MΦ. Moreover, peritumoral HSCs were related to more early recurrences. It is important to note that the density of peritumoral activated HSCs, in combination with seprase and osteonectin mRNA or density of Tregs and MΦ, might predict prognoses more effectively.*

Hepatocellular carcinoma (HCC) is one of the most common cancers worldwide.<sup>1</sup> More patients with HCC are being offered the option of resection as a curative strategy. Unfortunately, high rates of postoperative recurrence and metastasis remain major obstacles. It is well known that HCC, frequently the long-term result of chronic hepatitis and cirrhosis, is characterized by typical signs of inflammation, such as heavy infiltration by many leukocyte populations.<sup>2,3</sup> The hepatitis status and local inflammatory processes influence survival and recurrence in patients with HCC after curative resection.<sup>2,4</sup> Our group has identified that HCC metastasis was associated with not only the peritumoral inflammatory response but also with macrophage infiltration and the expression of macrophage colony-stimulating factor in peritumoral liver tissue.<sup>3,5</sup> Together with the fact that recurrences of HCC primarily target the liver itself,<sup>6</sup> it is logical to highlight that the peritumoral liver environment, especially the inflammation-related factors, is of prometastatic and prognostic significance and, hence, worthy of further investigation.

Hepatic stellate cells (HSCs), the versatile mesenchymal cells in the liver parenchyma, are vital to the liver's response to inflammation. Their activation into contractile myofibroblasts is the major pathway in hepatic fibrogenesis that resulted from chronic hepatitis.<sup>7</sup> Especially, the production of the putative functional genes of activated HSCs, including osteonectin (*SPARC*),<sup>8</sup> tenascin-C (*TNC*),<sup>9</sup> and seprase (*FAP*),<sup>10</sup> can modulate extracellular matrix, exacerbate chronic inflammation, and accelerate the process of fibrosis. However, the function of activated HSCs is not limited to chronic inflammation and subsequent liver fibrogenesis. They have also emerged as potent suppressors of hepatic

immunity<sup>11-13</sup> and promoters of neoangiogenesis during chronic hepatitis virus infection.<sup>14</sup> It is important to note that evidence from other cancers, such as gastrointestinal carcinomas and melanoma, has verified that host-activated HSCs contributed to the establishment of liver metastases via inflammatory response-related mechanisms.<sup>15-17</sup> In addition, myofibroblast-derived factors such as FAP and SPARC can otherwise accurately predict recurrence in colon and pancreatic cancers.<sup>18,19</sup> Therefore, it is conceivable that peritumoral activated HSCs may be significantly involved in the recurrence of HCC.

Preliminary *in vitro* and murine xenograft models have proved that HSCs could be activated by HCC cells<sup>20</sup> and directly promote the aggressiveness and progression of HCC cells.<sup>21,22</sup> Further insight into the involvement of activated HSCs in human HCC indicates that they can accumulate the intratumoral and peritumoral stroma of HCC.<sup>23,24</sup> However, all the cited studies are *in vitro* coculture assays, reconstitution in animal models, or *in situ* experiments providing no prognostic information. Therefore, the roles of functional genes and the cellular density of peritumoral activated HSCs in HCC progression and recurrence remain obscure, and systematic clinical studies are needed.

To this end, in a randomly selected cohort of patients with HCC, using *in situ* immunostaining and quantitative real-time polymerase chain reaction (qRT-PCR), we examined the prognostic value of peritumoral activated HSCs at the cellular and gene levels. Simultaneously, we also evaluated the density of peritumoral regulatory T cells (Tregs) and CD68+ macrophages (MΦ), which also contribute to hepatic immunoregulation and inflammation response. We found that peritumoral activated HSCs were independent predictors of a poorer prognosis in HCC.

## Materials and Methods

### Patient Samples

The inclusion and exclusion criteria included the following: (1) pathologically proved HCC; (2) no anticancer treatment or distant metastases before surgery; and (3) history of HCC resection, defined as macroscopically complete removal of the tumors, as previously described.<sup>2,4</sup> After institutional review board approval, 130 patients with HCC were randomly selected from a total of 1,905 patients in Zhongshan Hospital, Shanghai, the People's Republic of China, between 2002 and 2005, who had complete clinicopathologic and follow-up data and represented a prospective, continuous, unselected cohort of patients. Meanwhile, a normal liver tissue pool from 10 healthy liver donors was constructed as the calibrator for qRT-PCR reactions.

Clinical staging was performed according to the 2002 American Joint Committee on Cancer/International Union Against Cancer TNM staging system.<sup>25</sup> The histologic grade of tumor differentiation was determined by using the Edmondson grading system.<sup>26</sup> The pathologic features of all cases were rereviewed by a skilled pathologist who had no information about the original pathology reports. Liver function was assessed by using the Child-Pugh scoring system.<sup>27</sup> If patients had multiple lesions in the liver, we selected the main nodule for study.<sup>28</sup> In cases with tumors with different histologic grades, the most advanced grade was used. **Table 1** summarizes the conventional clinicopathologic parameters.

### Follow-up

All patients were monitored postoperatively until September 30, 2008, by serum  $\alpha$ -fetoprotein (AFP), abdominal ultrasonography, and chest radiograph every 1 to 6 months according to the postoperative time. For patients with test results suggestive of recurrence, computed tomography and/or magnetic resonance imaging were used to verify whether recurrence had occurred. Recurrences were confirmed based on typical imaging appearances in computed tomography scans and/or magnetic resonance imaging and an elevated AFP level.<sup>2</sup> The mean  $\pm$  SE follow-up period was  $31.8 \pm 1.7$  months (range, 1.5-77.0 months). Recurrence-free survival (RFS) was the time between surgery and first confirmed relapse. If recurrence was not diagnosed at the time of study, the cases were censored on the date of death or of the last follow-up. Of the 130 patients, 68 were confirmed as having relapse, including 60 intrahepatic recurrences and 8 extrahepatic metastases. Postrecurrence treatments (reoperation [n = 12], chemoembolization [n = 34], and regional therapy [n = 3]) and surveillance according to a uniform guideline were described previously.<sup>2,4</sup> However, 19 patients with recurrence with severe liver dysfunction or weak general performance could not tolerate antirecurrence treatments. Overall survival (OS) was defined as the interval between surgery and death or between surgery and the last follow-up for surviving patients. Of the patients, 71 died as a result of recurrence (n = 51) or complicated liver cirrhosis (n = 20).

### Tissue Microarrays and Immunohistochemical Analysis

Tissue microarrays were constructed as described previously.<sup>2</sup> Triplicates of 1-mm-diameter cylinders (0.785 mm<sup>2</sup>) from a noncancerous margin (designated as peritumor) were included in each case, together with different control samples that ensured reproducibility and homogeneous staining (Shanghai Biochip, Shanghai). Thus, 2 tissue microarray blocks were constructed, each containing 204 cylinders, including 9 different control samples. Serial sections (4  $\mu$ m) were placed on slides coated with 3-aminopropyltriethoxysilane.

Mouse antihuman  $\alpha$ -smooth muscle actin ( $\alpha$ -SMA) (dilution 1:100; DAKO, Carpinteria, CA), Foxp3 (dilution 1:100; AbD Serotec, Kidlington, England), and CD68 (dilution 1:100; Zymed Laboratories, San Francisco, CA) monoclonal antibodies were used. According to the guidelines, the positive control pool comprised blood vessels for  $\alpha$ -SMA and tonsil or spleen for Foxp3 and CD68. In addition, normal liver tissues were used as normal control samples. Immunohistochemical analysis was performed using a 2-step protocol (Novolink Polymer Detection System, Novocastra, Newcastle upon Tyne, England) as described previously.<sup>29</sup> Briefly, sections were deparaffinized, hydrated, and washed. After neutralization of endogenous peroxidase and microwave antigen retrieval, slides were preincubated with blocking serum and then incubated overnight with primary antibodies. Subsequently, the sections were serially rinsed, incubated with second antibodies, and treated with horseradish peroxidase-conjugated streptavidin. Reaction products were developed with 3,3'-di-

aminobenzidine solution and counterstained with hematoxylin. Negative control slides, in which incubation with the primary antibody was omitted, were included in all assays.

The number of stained cells was counted ( $\times 400$ ) using a computerized image-analysis system composed of a Leica DFC420 CCD camera, installed on a Leica DMIRE2 light microscope (Leica Microsystems, Wetzlar, Germany) and attached to a personal computer. The entire disk of each triplicate was selected for enumeration. Data were expressed as the mean ( $\pm$  SE) number of cells (ie, cell density per 0.785 mm<sup>2</sup>), based on the triplicate samples obtained from each patient.

Activated HSCs were identified by their location, morphologic features, and cytoplasmic expression of  $\alpha$ -SMA.<sup>12</sup> Areas of vessels, Glisson capsules, fibrous septa, and collapsed parenchyma were not assessed.<sup>30</sup> M $\Phi$  were stained brown in the cytoplasm by anti-CD68 antibody,<sup>31</sup> and Tregs were verified by their distinct nuclear staining of Foxp3.<sup>2</sup>

**Table 1**  
Clinicopathologic Characteristics in 130 Cases of Hepatocellular Carcinoma

Characteristic	No. (%)	Characteristic	No. (%)
Sex		History of hepatitis	
Male	112 (86.2)	No	10 (7.7)
Female	18 (13.8)	Yes	120 (92.3)
Age (y)		Hepatitis B e antigen	
$\leq 52$	67 (51.5)	Negative	87 (66.9)
$> 52$	63 (48.5)	Positive	32 (24.6)
Tumor size (cm)		No HBV infection	11 (8.5)
$\leq 5$	62 (47.7)	Hepatitis B surface antigen	
$> 5$	68 (52.3)	Negative	8 (6.2)
No. of tumors		Positive	111 (85.4)
1	101 (77.7)	No HBV infection	11 (8.5)
$\geq 2$	29 (22.3)	Partial thromboplastin time (s)	
Vascular invasion		$\leq 13$	109 (83.8)
No	71 (54.6)	$> 13$	21 (16.2)
Yes	59 (45.4)	Alanine aminotransferase, U/L ( $\mu$ kat/L)	
Encapsulation		$\leq 80$ (1.34)	68 (52.3)
Yes	60 (46.2)	$> 80$ (1.34)	62 (47.7)
No	70 (53.8)	Albumin, g/dL (g/L)	
Differentiation		$\geq 3.5$ (35)	122 (93.8)
I-II	66 (50.8)	$< 3.5$ (35)	8 (6.2)
III-IV	64 (49.2)	Child-Pugh score A	130 (100.0)
Cirrhosis		Postoperative prophylactic treatment	
No	19 (14.6)	None	52 (40.0)
Yes	111 (85.4)	TACE	64 (49.2)
TNM stage		Immunotherapy*	14 (10.8)
I	74 (56.9)	Postrecurrence therapy (n = 68)	
II-III	56 (43.1)	Reresection	12 (17.6)
$\alpha$ -Fetoprotein, ng/mL ( $\mu$ g/L)		TACE	34 (50.0)
$\leq 20$ (20)	49 (37.7)	Regional therapy†	3 (4.4)
$> 20$ (20)	81 (62.3)	None	19 (28.0)
Total bilirubin, mg/dL ( $\mu$ mol/L)		Outcome	
$\leq 1.0$ (17.1)	80 (61.5)	Died	71 (54.6)
$> 1.0$ (17.1)	50 (38.5)	Alive	59 (45.4)
$\gamma$ -Glutamyltransferase, U/L ( $\mu$ kat/L)		Recurrence	
$\leq 54$ (0.90)	52 (40.0)	No	62 (47.7)
$> 54$ (0.90)	78 (60.0)	Yes	68 (52.3)

HBV, hepatitis B virus; TACE, transcatheter arterial chemoembolization.

\* Including interleukin-1, interferon- $\gamma$ , or thymic peptide therapy.

† Including radiotherapy, radiofrequency therapy, etc.

Two independent investigators blinded to the clinicopathologic data assessed the numbers of these cells. Variations in counts that exceeded 5% were reevaluated, and a consensus decision was made.

### Quantitative RT-PCR

*SPARC*, *FAP*, and *TNC*, all mainly expressed by activated HSCs in the liver, were selected as candidate functional genes. Hypoxanthine phosphoribosyltransferase 1 (*HPRT1*) and TATA box binding protein (*TBP*) were used

as housekeeping genes, as described previously.<sup>32</sup> Primers for these genes are listed in **Table 2**. Total RNA was extracted by using TRIzol (Invitrogen, Carlsbad, CA) purified with the RNeasy Mini Kit (Qiagen, Valencia, CA) and retrotranscribed by oligo (dT)<sub>18</sub> primers and Super-Script III Reverse Transcriptase (Invitrogen). Genomic DNA contamination was eliminated by using DNaseI. The mean  $\pm$  SE A260/280 ratio of the RNA samples was  $2.07 \pm 0.006$  (range, 1.80-2.21). RNA integrity was characterized by the 28S/18S ratio ( $>1.5$ ) on 1% agarose gels **Image 1A**. For qRT-PCR experiments,

**Table 2**  
Primer Sequences for Quantitative Real-Time Polymerase Chain Reaction in 130 Cases of Hepatocellular Carcinoma

Target Messenger RNA/Primer Sequence (US/DS)	Annealing Temperature (°C)	Fragment Amplified (bp)
<i>TNC</i> 5'-CAAGTTCAGCGTGGGAGATG-3' 5'-ACTGGATTGAGTGTTCTGGGC-3'	60	278
<i>SPARC</i> 5'-CATAAGCCCAGTTCATCACCA-3' 5'-ACAACCGATTCACTCACTCCA-3'	60	277
<i>FAP</i> 5'-TCAACTGTGATGGCAAGAGCA-3' 5'-TAGGAAGTGGGTCATGTGGGT-3'	60	219
<i>HPRT1</i> 5'-CCTGGCGTCGTGATTAGTG-3' 5'-CAGAGGGCTACAATGTGATGG-3'	60	182
<i>TBP</i> 5'-ACCACTCCACTGTATCCCTCC-3' 5'-CTGTTCTCACTCTTGGCTCCT-3'	60	285

bp, base pairs; *FAP*, seprase; *HPRT1*, hypoxanthine phosphoribosyltransferase 1; *SPARC*, osteonectin; *TBP*, TATA box binding protein; *TNC*, tenascin-C; US/DS, upstream sequence/downstream sequence.

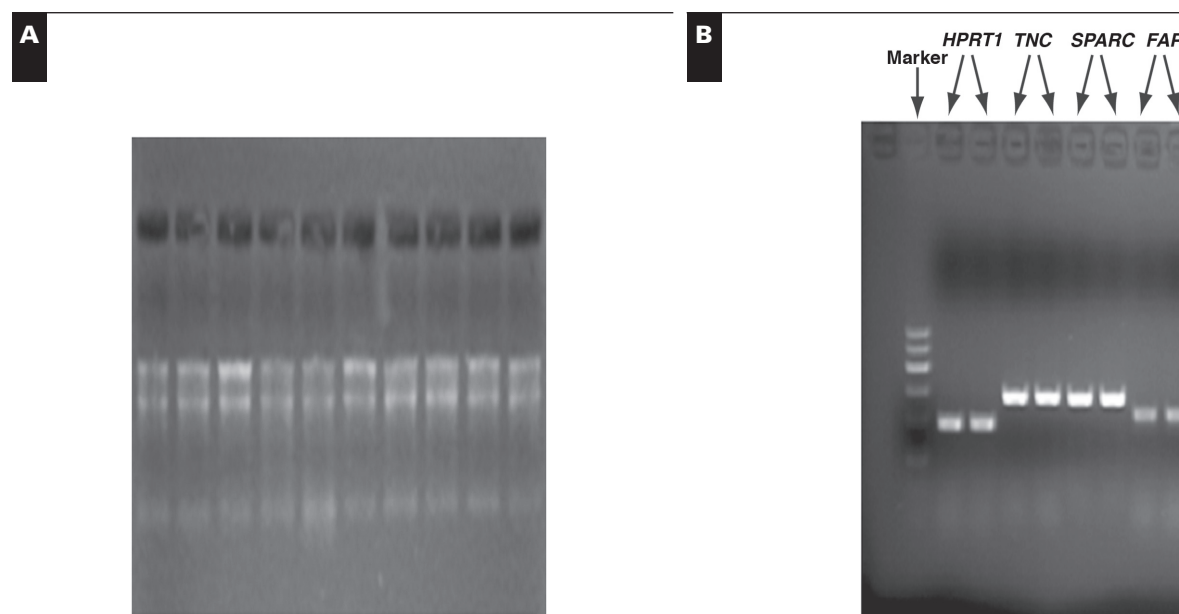
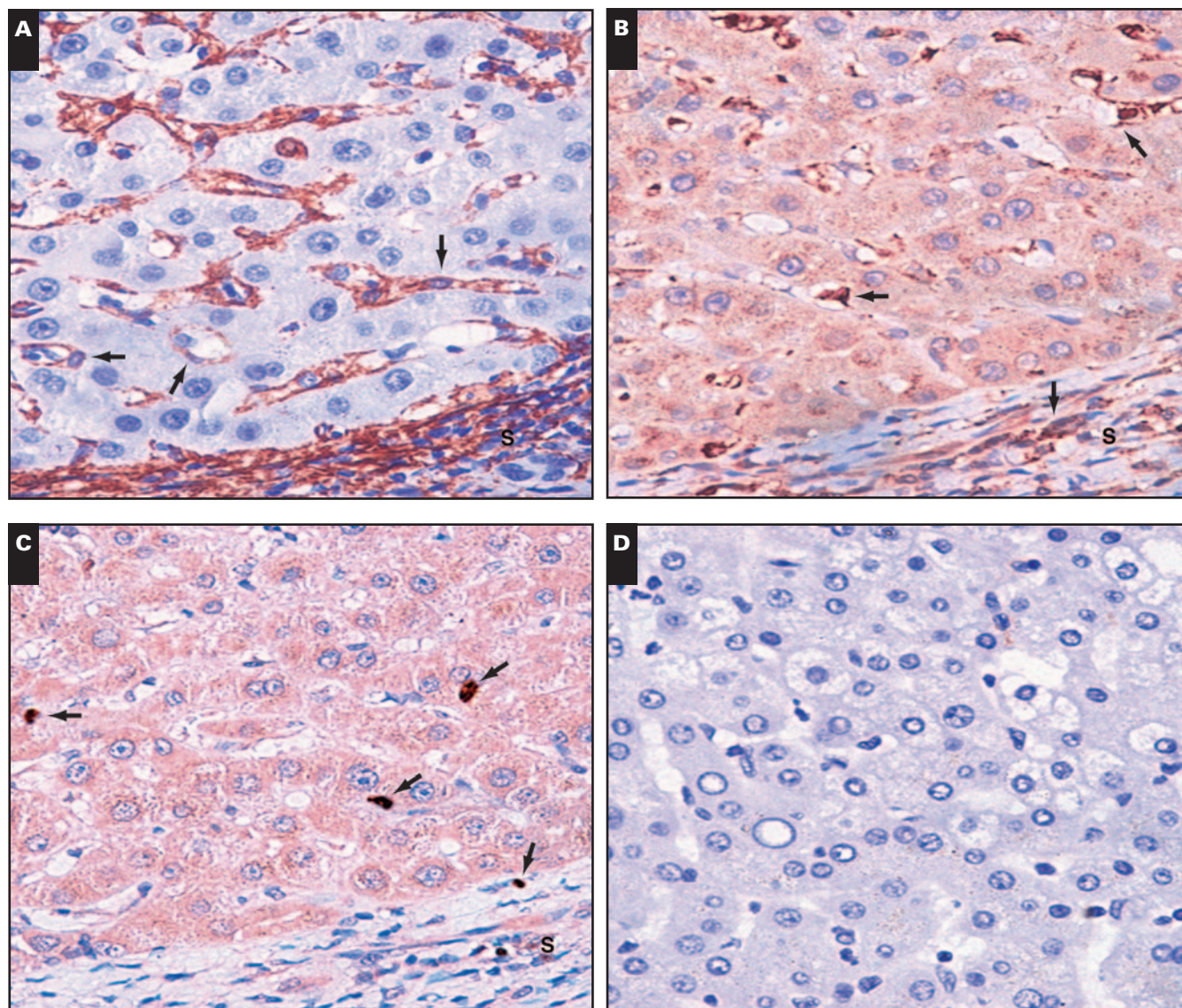


**Image 1** Electrophoresis of RNA integrity analysis and polymerase chain reaction (PCR) products. The integrity of purified RNA samples was confirmed by electrophoresis on 1% agarose gels. **A**, High-quality RNA samples were characterized by 28S/18S ratios greater than 1.5 on a 1% agarose gel and sharp bands. **B**, PCR products were loaded on a 2% agarose gel to confirm specific gene amplification, demonstrated by a single sharp band of the appropriate size.



an ABI Prism 7900 SDS (Applied Biosystems, Foster City, CA) and SYBR Green PCR Master Mix (SuperArray, now SABiosciences, Frederick, MD). For all samples, RNA was analyzed in duplicate. The amount of complementary DNA was the same for each reaction. The PCR products were run on a 2% agarose gel to confirm specific gene amplification and the absence of primer dimers **Image 1B**. For data analysis, the  $2^{-\Delta\Delta C_t}$  method was used.<sup>33</sup> The fold change in the target genes, normalized to average housekeeping genes and calibrated to the expression of the normal liver pool (n = 10), was calculated for each sample.

### Statistics

Data were analyzed using SPSS software, version 15.0 (SPSS, Chicago, IL). Cumulative survival was calculated by using the Kaplan-Meier method and compared by log-rank test. Multivariate analyzing was performed by using the Cox

multivariate proportional hazards regression model. The optimal cutoff values, estimated by using X-tile software, version 3.6.1 (Yale University, New Haven, CT),<sup>34</sup> were 25%, 25%, 20%, 35%, 35%, and 30% for activated HSCs, Foxp3+ Tregs, MΦ, *FAP*, *SPARC*, and *TNC*, respectively. For the comparison of variables,  $\chi^2$  tests, Fisher exact tests, Spearman *r* coefficient tests, and Mann-Whitney *U* tests were carried out as appropriate. A *P* value of less than .05 was considered statistically significant.

## Results

### Immunohistochemical Characteristics

The triplicate of spots for each case showed a good level of homogeneity for stained cell density. Representative images **Image 2** and statistics for immunohistochemical

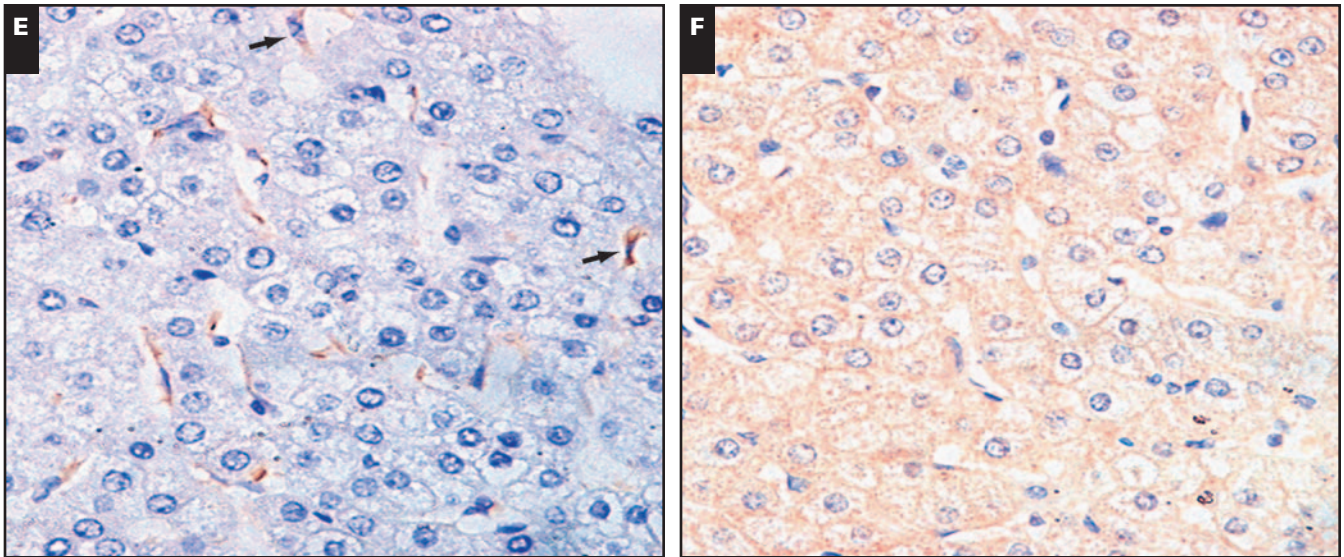


**Image 2** Images of immunostained cells. Representative images for immunohistochemical study on activated hepatic stellate cells (HSCs) (**A** and **D**), CD68+ macrophages (**B** and **E**), and Foxp3+ regulatory T cells (**C** and **F**). **A**, **B**, and **C** (Case 64), All high. **D**, **E**, and **F** (Case 105), All low. For HSC evaluation, areas with fibrous septa (S) were not examined (**A-F**,  $\times 400$ ). Arrows indicate representative cells.

variables are shown **Table 3**. Infiltration of Tregs or M $\Phi$  increased together with the accumulation of peritumoral activated HSCs. The number of activated HSCs correlated in a linear way to that of Tregs ( $r = 0.285$ ;  $P = .001$ ) and M $\Phi$  ( $r = 0.273$ ;  $P = .029$ ).

### Profiles of Genes Related to Activated HSC Function

The expression levels of *FAP*, *SPARC*, and *TNC* significantly correlated with one another ( $r = 0.824$ ,  $r = 0.624$ , and  $r = 0.614$ , respectively; all  $P < .0001$ ) and with the density of activated HSCs ( $r = 0.903$ ,  $r = 0.634$ , and  $r = 0.887$ , respectively; all  $P < .0001$ ). In addition, their expression differed dramatically between high- and low-density activated HSCs subgroups (all  $P < .001$ ). Compared with expression level in normal liver tissues, the mean expression levels of *FAP*, *SPARC*, and *TNC* were higher in peritumoral tissue (Table 3).

### Prognostic Factors

For the entire study cohort, the OS and RFS rates were 78.5% and 64.0% at 1 year, 50.3% and 45.3% at 3 years, and 43.0% and 41.4% at 5 years. Compared with patients without recurrence, patients with recurrence had dismal 5-year OS rates (17.7% vs 72.4%;  $P < .001$ ).

The density of peritumoral activated HSCs correlated inversely with OS and RFS in univariate statistics **Table 4**. The 5-year OS and RFS rates for high- vs low-density peritumoral activated HSCs were 31.8% vs 77.8% ( $P = .001$ ) **Figure 1A** and 28.0% vs 77.3% ( $P < .001$ ) **Figure 1B**, respectively. Dismal OS and RFS, respectively, also related

**Table 3** Statistics for Number of Peritumoral Activated HSCs, Tregs, and M $\Phi$  and Functional Genes Expression Levels in HSCs in 130 Cases of Hepatocellular Carcinoma

	Mean $\pm$ SE	Range
No. of cells		
Activated HSCs	145.06 $\pm$ 9.38	7.00-515.75
Tregs	13.71 $\pm$ 1.70	0.33-142.67
M $\Phi$	319.05 $\pm$ 18.25	0.00-1,121.00
mRNA expression (fold change)		
<i>FAP</i>	4.10 $\pm$ 0.35	0.23-18.51
<i>SPARC</i>	5.69 $\pm$ 0.33	0.08-18.64
<i>TNC</i>	1.79 $\pm$ 0.12	0.07-7.78

*FAP*, seprase; HSCs, hepatic stellate cells; mRNA, messenger RNA; M $\Phi$ , CD68+ macrophages; *SPARC*, osteonectin; *TNC*, tenascin-C; Tregs, Foxp3+ regulatory T cells.

to high levels of M $\Phi$  ( $P = .001$  and  $P = .020$ ), Tregs ( $P = .010$  and  $P = .009$ ), *SPARC* ( $P = .002$  and  $P = .002$ ), *FAP* ( $P = .005$  and  $P < .001$ ), and *TNC* ( $P = .014$  and  $P = .003$ ).

The statistically significant variables were further included in multivariate analyses (Table 4). High-density peritumoral activated HSCs, M $\Phi$ , and Tregs remained as independent predictors of survival or recurrence, as did *SPARC* messenger RNA (mRNA) expression. *FAP* mRNA expression was associated only with RFS.

With 1 year as the cutoff period, all recurrences were divided into early recurrence, which is mainly from disseminated tumor cells, and late recurrence, usually a result of a multicentric new tumor.<sup>35</sup> Prominent differences in median

**Table 4**  
**Analyses for Recurrence and Survival in 130 Cases of Hepatocellular Carcinoma\***

Factor	Overall Survival				Recurrence-Free Survival			
	Univariate Analysis		Multivariate Analysis		Univariate Analysis		Multivariate Analysis	
	P	Hazard Ratio	95% CI	P	P	Hazard Ratio	95% CI	P
Age, y (≤52 vs >52)	NS			NA	NS			NA
Sex (female vs male)	NS			NA	NS			NA
Hepatitis history (no vs yes)	NS			NA	NS			NA
HBsAg (positive vs negative vs no HBV)	NS			NA	NS			NA
HBeAg (positive vs negative vs no HBV)	NS			NA	NS			NA
Liver cirrhosis (no vs yes)	NS			NA	NS			NA
ALT, U/L (≤80 vs >80)	NS			NA	NS			NA
Tumor differentiation (I-II vs III-IV)	.007			NS	NS			NA
Tumor size, cm (≤5 vs >5)	<.001			NS	<.001			NS
No. of tumors (1 vs ≥2)	NS			NA	<.001	1.903	1.177-3.079	.009
Tumor encapsulation (complete vs none)	.007			NS	<.001			NS
Vascular invasion (no vs yes)	<.001	2.057	1.101-3.844	.024	<.001	2.561	1.505-4.358	.001
TNM stage (I vs II-III)	<.001	2.718	1.484-4.977	.001	<.001			NS
AFP, μg/L (≤400 vs >400)	.001			NS	.001			NS
PTT, s (≤13 vs >13)	NS			NA	NS			NA
Albumin, g/L (≥35 vs <35)	NS			NA	NS			NA
Total bilirubin, μmol/L (≤17.1 vs >17.1)	NS			NA	NS			NA
GGT, U/L (≤54 vs >54)	.003			NS	NS			NA
Peritumoral features (low vs high)								
Activated HSCs	.001	2.632	1.157-5.986	.021	<.001	3.331	1.388-7.997	.007
MΦ	.001	4.265	1.654-10.999	.003	.020	2.537	1.192-5.398	.016
Tregs	.010	2.377	1.115-5.067	.025	.009	2.347	1.156-4.763	.018
SPARC	.002	2.081	1.114-3.887	.021	.002	2.353	1.261-4.390	.007
FAP	.005			NS	<.001	3.453	1.687-7.069	.001
TNC	.014			NS	.003			NS
Combinations (I vs II vs III vs IV) of activated HSCs and								
Tregs	.001	1.667	1.190-2.337	.003	<.001	1.721	1.237-2.395	.001
MΦ	<.001	2.061	1.375-3.089	.001	<.001	1.693	1.218-2.355	.002
SPARC	.007	1.355	1.064-1.725	.014	.001	1.438	1.126-1.836	.004
FAP	NA			NA	<.001	1.643	1.242-2.172	<.001

AFP, α-fetoprotein; ALT, alanine aminotransferase; CI, confidence interval; FAP, seprase; GGT, γ-glutamyltransferase; HBeAg, hepatitis B e antigen; HBsAg, hepatitis B surface antigen; HBV, hepatitis B virus; HSC, hepatic stellate cell; MΦ, CD68+ macrophages; NA, not adopted; NS, not significant; PTT, partial thromboplastin time; SPARC, osteonectin; TNC, tenascin-C; Tregs, regulatory T cells.

\* Univariate analysis, Kaplan-Meier, log-rank test; multivariate analysis, Cox multivariate proportional hazards regression model. Values for ALT and GGT are given in conventional units; Système International (SI) units are as follows: ALT, ≤1.34 vs >1.34 μkat/L; GGT, ≤0.90 vs >0.90 μkat/L. Values for AFP, albumin, and total bilirubin are given in SI units; conventional units are as follows: AFP, ≤400 vs >400 ng/mL; albumin, ≥3.5 vs <3.5 g/dL; and total bilirubin, ≤1.0 vs >1.0 mg/dL.

OS (16.1 vs 59.2 months;  $P < .001$ ) and postrecurrence survival (9.5 vs 30.0 months;  $P = .004$ ) were estimated between early and late recurrence. Patients with high-density HSCs in the peritumoral area or high SPARC or high FAP mRNA levels significantly suffered more early recurrence (44/98 vs 5/32 [ $P = .003$ ]; 38/85 vs 11/45 [ $P = .023$ ]; 41/85 vs 8/45 [ $P = .001$ ], respectively) than late recurrence (17/98 vs 2/32 [ $P = .156$ ]; 15/85 vs 4/45 [ $P = .179$ ]; 16/85 vs 3/45 [ $P = .062$ ], respectively) compared with patients with low-density HSCs or low SPARC or low FAP mRNA levels.

It should be noted that the distributions of postoperative prophylactic treatments and postrecurrence therapies were equivalent between high and low subgroups of HSC density, MΦ density, Treg density, SPARC level, and FAP level, indicating that the therapeutic modalities produced no obscuring effects for the analyses **Table 5**.

### Combination of the Density of Peritumoral Activated HSCs and Other Investigated Variables With Prognostic Value and Receiver Operating Curve Analysis

Whenever peritumoral MΦ and Treg density and the mRNA levels of FAP and SPARC had independent prognostic value, the results were combined with results for the density of peritumoral activated HSCs in turn. Each combination comprised 4 subgroups: I, both low; II, only HSCs high; III, only HSCs low; and IV, both high. The corresponding numbers of cases for the 4 subgroups (I/II/III/IV) of the combinations for density of activated HSCs with MΦ density, Treg density, FAP mRNA level, and SPARC mRNA level were as follows: 10/16/22/82, 10/21/22/77, 28/17/4/81, and 31/14/1/84, respectively. OS could be perfectly predicted by the combinations for density of HSCs with SPARC, Tregs, and MΦ **Figure 1C**; RFS was

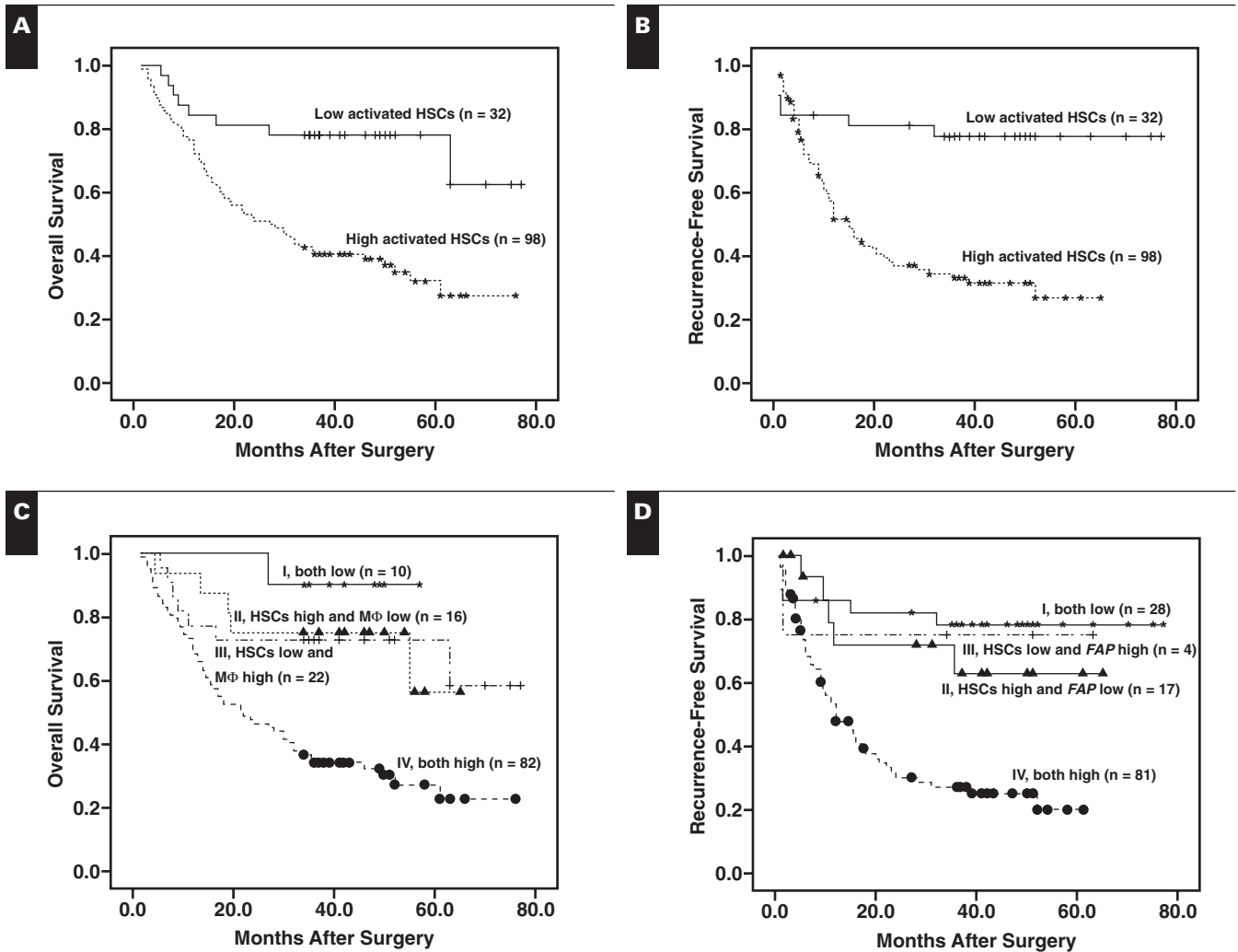


**Figure 1** Survival curves for univariate analyses. Kaplan-Meier analyses for peritumoral activated hepatic stellate cells (HSCs; **A** and **B**) and combinations of peritumoral activated HSCs with CD68+ macrophages (MΦ; **C**), or seprase (*FAP*; **D**) were selected as deputies for univariate analyses of overall survival (**A** and **C**) and recurrence-free survival (**B** and **D**). **A**,  $P = .001$ . **B**,  $P < .001$ . **C**, Overall  $P < .001$ ; I vs II,  $P = .336$ ; I vs III,  $P = .258$ ; I vs IV,  $P = .008$ ; II vs III,  $P = .797$ ; II vs IV,  $P = .007$ ; and III vs IV,  $P = .006$ . **D**, Overall  $P < .001$ ; I vs II,  $P = .332$ ; I vs III,  $P = .770$ ; I vs IV,  $P < .001$ ; II vs III,  $P = .805$ ; II vs IV,  $P = .009$ ; and III vs IV,  $P = .135$ .

significantly associated with the combinations of HSCs with Tregs, MΦ, *SPARC*, and *FAP* (Figure 1D).

All independent prognostic parameters were then compared by receiver operating characteristic analyses. The best predictive value for recurrence was the combination of the density of peritumoral activated HSCs and the *FAP* mRNA level. The area under the curve of this combination was 0.721 for RFS (Table 6) and (Figure 2A). However, vascular invasion was the best predictor for OS.

### Correlations Between Independent Prognostic Markers and Clinicopathologic Features

As shown in Table 5, patients with high-density peritumoral activated HSCs were prone to have larger tumors,

high rates of vascular invasion, no encapsulation, advanced TNM stage, and a higher serum AFP level. In particular, the status of hepatitis B surface antigen (positive, negative, or no hepatitis B infection) had an unbalanced distribution between patients with high- and low-density activated HSCs ( $P = .037$ ). With respect to the functional genes of activated HSCs, we found that high *SPARC* and *FAP* expression correlated with larger tumors and higher serum AFP levels. Moreover, vascular invasion, no encapsulation, advanced TNM stage, and higher serum  $\gamma$ -glutamyltransferase levels were associated with high *FAP* expression. In addition, patients with high MΦ density had higher rates of vascular invasion. Younger patients and patients with vascular invasion had more peritumoral Treg infiltration.



**Table 5**  
**Correlation of Peritumoral MΦ, HSC, and Treg Density and SPARC and FAP mRNA Expression Levels With Clinicopathologic**

Variable	HSCs			MΦ			Tregs		
	Low (n = 32)	High (n = 98)	P	Low (n = 26)	High (n = 104)	P	Low (n = 31)	High (n = 99)	P
Age (y)			.155			.054			.04
≤52	13	54		9	58		11	56	
>52	19	44		17	46		20	43	
Sex†			.771			.525			.766
M	27	85		21	91		26	86	
F	5	13		5	13		5	13	
Tumor size (cm)			.002			.114			.185
≤5	23	39		16	46		18	44	
>5	9	59		10	58		13	55	
No. of tumors			.674			.092			.967
1	24	77		17	84		24	77	
≥2	8	21		9	20		7	22	
Vascular invasion			.024			.035			.036
No	23	48		19	52		22	49	
Yes	9	50		7	52		9	50	
Encapsulation			.011			.187			.485
Yes	21	39		15	45		16	44	
No	11	59		11	59		15	55	
Differentiation			.612			.035			.604
I-II	15	51		18	48		17	49	
III-IV	17	47		8	56		14	50	
Cirrhosis			.852			.901			.392
No	5	14		4	15		6	13	
Yes	27	84		22	89		25	86	
TNM stage			.049			.595			.883
I	23	51		16	58		18	56	
II-III	9	47		10	46		13	43	
HBsAg‡			.037			1.000			.246
Negative	5	3		2	6		2	6	
Positive	25	86		22	89		24	87	
No HBV	2	9		2	9		5	6	
HBeAg			.569			.745			.190
Negative	20	67		19	68		20	67	
Positive	10	22		5	27		6	26	
No HBV	2	9		2	9		5	6	
Hepatitis‡			1.000			1.000			.249
No	2	8		2	8		4	6	
Yes	30	90		24	96		27	93	
Mean AFP (μg/L)‡	2,167.8	7,324.7	.02	4,123.4	6,538.3	.473	3,952.9	6,713.6	.382
Mean ALT (U/L)‡	44.5	7.7	.395	43.4	69.4	.433	54.6	67.2	.684
Mean TBil (μmol/L)‡	17.1	18.3	.693	16.8	18.4	.633	17.7	18.1	.664
Mean albumin (g/L)‡	48.4	41.5	.084	41.6	41.9	.933	43.0	41.4	.108
Mean GGT (U/L)‡	75.9	106.9	.207	69.8	106.7	.162	79.5	105.5	.295
Postoperative prophylactic treatment (n = 130)			.658			.554			.209
None	15	37		8	44		11	41	
TACE	14	50		15	49		14	50	
Immunotherapy§	3	11		3	11		6	8	
Postrecurrence treatment (n = 68)†			.481			.310			.245
None	2	17		1	18		3	16	
TACE	5	29		8	26		2	32	
Local therapy	0	3		0	3		0	3	
Reoperation	0	12		2	10		3	9	

AFP, α-fetoprotein; ALT, alanine aminotransferase; FAP, seprase; GGT, γ-glutamyltransferase; HBeAg, hepatitis B e antigen; HBsAg, hepatitis B surface antigen; HBV, hepatitis B virus; HSCs, hepatic stellate cells; MΦ, CD68+ macrophages; SPARC, osteonectin; TACE, transcatheter arterial chemoembolization; TBil, total bilirubin; Tregs, Foxp3+ regulatory T cells.

\* Values for ALT and GGT are given in conventional units; conversions to Système International (SI) units are as follows: ALT (μkat/L), multiply by 0.0167; GGT (μkat/L), multiply by 0.01667. Values for AFP, albumin, and total bilirubin are given in SI units; conversions to conventional units are as follows: AFP (ng/mL), divide by 1.0; albumin (g/dL), divide by 10; and total bilirubin (mg/dL), divide by 17.104. P values were evaluated by χ² tests unless otherwise indicated.

† Fisher exact test.

‡ Mann-Whitney U test.

§ Including interleukin-1, interferon-γ, or thymic peptide therapy.

|| Including radiotherapy, radiofrequency therapy, etc.

Downloaded from https://academic.oup.com/ajcp/article/131/4/498/1760512 by guest on 24 April 2024

Features and Therapy in 130 Cases of Hepatocellular Carcinoma\*

SPARC			FAP		
Low (n = 45)	High (n = 85)	P	Low (n = 45)	High (n = 85)	P
24	43	.766	24	43	.766
21	42		21	42	
39	73	.902	39	73	.902
6	12		6	12	
27	35	.041	31	31	.0004
18	50		14	54	
32	69	.19	33	68	.385
13	16		12	17	
27	44	.37	31	40	.017
18	41		14	45	
24	36	.232	28	32	.007
21	49		17	53	
21	45	.496	23	43	.955
24	40		22	42	
7	12	.825	7	12	.825
38	73		38	73	
30	44	.103	32	42	.017
15	41		13	43	
5	3	.133	5	3	.133
38	73		38	73	
2	9	.402	2	9	.474
30	57		32	55	
13	19	.492	11	21	.492
2	9		2	9	
2	8		2	8	
43	77		43	77	
1,852.5	828.3	.004	1,796.9	8,309.8	.003
43.6	75.1	.257	8.2	55.8	.38
16.6	18.8	.967	15.8	19.2	.330
42.4	41.5	.295	42.8	41.3	.061
72.3	113.6	.062	69.6	115.1	.04
		.855			.995
19	33		18	34	
22	42		22	42	
4	10	.740	5	9	.234
4	15		1	18	
9	25		8	26	
0	3		1	2	
2	10		1	11	

## Discussion

Our study provides the first significant prognostic relevance of peritumoral activated HSCs in HCC. Compared with patients with low-density activated HSCs, patients with high-density peritumoral activated HSCs have significant dismal clinical outcomes (median OS, 26.5 vs 60.0

months [ $P = .001$ ], Figure 1A; median RFS, 16.8 vs 60.0 months [ $P < .001$ ], Figure 1B). We also found that higher mRNA expression levels of the functional genes of activated HSCs, such as *FAP* and *SPARC*, are independent predictors of poorer survival (for *SPARC*,  $P = .021$ , Table 4) and/or enhanced recurrence (for *SPARC*,  $P = .007$ ; for *FAP*,  $P = .001$ ; Table 4). In particular, combining the density for HSCs with the *SPARC* or *FAP* expression level yields better predictive performance. Besides, high levels of density and functional gene expression of peritumoral activated HSCs are associated with aggressive clinicopathologic characteristics such as larger tumors, high vascular invasion rates, no encapsulation, advanced TNM stage, and elevated AFP levels (Table 5). Collectively, based on cellular counting and functional gene analyses, peritumoral activated HSCs may serve as a significant prognosticator for a dismal outcome.

The peritumoral liver tissue is indisputably the principal target organ for HCC recurrence.<sup>6</sup> Notably, there are 2 categories of intrahepatic recurrences: one is intrahepatic micrometastases (IM) from the primary tumor, and the other is multicentric occurrence (MO). Although it is still difficult to accurately discriminate between IM and MO, documented evidence has suggested that IM mostly occurs as early recurrence ( $\leq 1$  year) after surgery, whereas MO usually seems to be a late recurrence ( $> 1$  year).<sup>35,36</sup> In the present study, more patients were identified as having early recurrence, a probable condition of having IM ( $n = 49$ ) and their postrecurrence survival was significantly inferior to that of patients with late recurrence ( $n = 19$ ) (9.5 vs 30.0 months;  $P = .004$ ). In addition, patients with higher density or higher functional gene levels of peritumoral activated HSCs have an increased incidence of IM compared with patients with lower density or gene levels. However, no relationship of peritumoral activated HSCs or functional gene expression level with MO was detected. Hence, we propose that the prognostic significance of peritumoral activated HSCs is mainly attributed to their role in promoting development and progression of IM, and the peritumoral liver tissue, if endowed with abundant activated HSCs, may serve as a fertile “soil” for micrometastases.

We found that *FAP*, *SPARC*, and *TNC* mRNA expression levels were positively correlated with the density of peritumoral activated HSCs, and the mean  $\pm$  SE fold changes of these genes were more than 1 ( $4.10 \pm 0.35$ ,  $5.69 \pm 0.33$ , and  $1.79 \pm 0.12$ , respectively) when calibrated against the normal liver tissue pool, suggesting that activated HSCs have an elevated expression level of these functional genes when the liver tissues are undergoing inflammation. Consequently, activated HSCs can synthesize more protein production of these genes to accelerate liver fibrosis.<sup>8-10,37</sup> Moreover, high *FAP* expression level of peritumoral activated HSCs is correlated with an enhanced serum  $\gamma$ -glutamyltransferase level

**Table 6**  
**Predictive Values for RFS and OS in 130 Cases of Hepatocellular Carcinoma**

Variable	RFS			OS		
	AUC	95% CI	P	AUC	95% CI	P
No. of tumors	0.597	0.499-0.694	.057			NA
Vascular invasion	0.709	0.619-0.799	<.001	0.729	0.640-0.819	<.001
TNM stage			NA	0.724	0.635-0.813	<.001
Peritumoral activated HSCs	0.658	0.563-0.752	.002	0.642	0.547-0.738	.005
Peritumoral activated Tregs	0.588	0.490-0.687	.082	0.604	0.506-0.701	.041
Peritumoral activated MΦ	0.565	0.466-0.664	.204	0.626	0.530-0.723	.013
FAP mRNA	0.698	0.606-0.789	<.001			NA
SPARC mRNA	0.636	0.540-0.732	.007	0.652	0.556-0.747	.003
Combined activated HSCs and Tregs	0.676	0.583-0.768	.001	0.681	0.588-0.773	<.001
MΦ	0.650	0.555-0.754	.003	0.714	0.624-0.804	<.001
FAP	0.721	0.631-0.810	<.001			NA
SPARC	0.662	0.567-0.756	.001	0.668	0.574-0.762	.001

AUC, area under the curve; CI, confidence interval; FAP, seprase; HSCs, hepatic stellate cells; mRNA, messenger RNA; MΦ, CD68+ macrophages; NA, not adopted because the corresponding variables were not independently associated with OS or RFS in multivariate analysis; OS, overall survival; RFS, recurrence-free survival; SPARC, osteonectin; Tregs, Foxp3+ regulatory T cells.

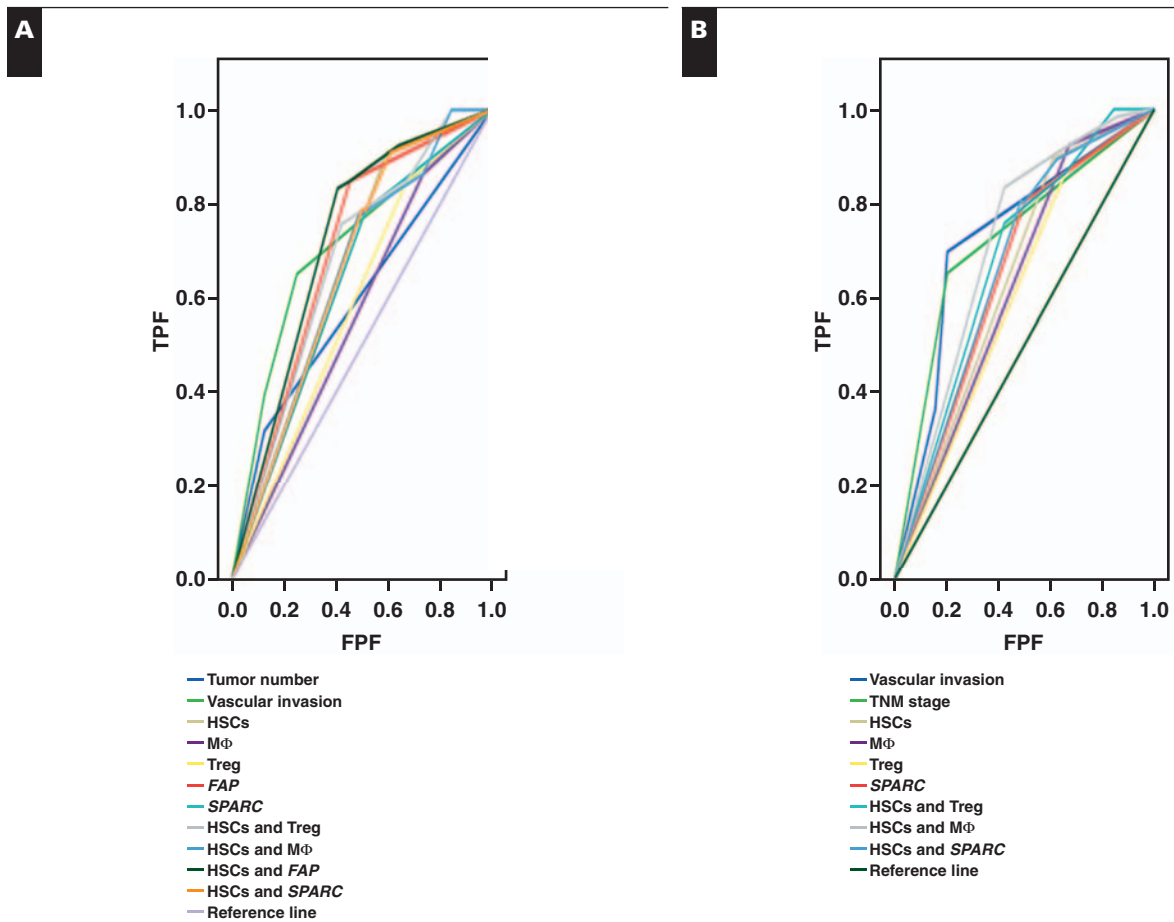


**Figure 2** Receiver operating characteristic analysis showed that the predictive effect of the combination of peritumoral activated hepatic stellate cells (HSCs) and seprase (FAP) messenger RNA expression for recurrence was best (A); however, no combination was better than vascular invasion in the prediction of overall survival (B). Comb, combined; FPF, false-positive fraction; MΦ, CD68+ macrophages; SPARC, osteonectin; TPF, true-positive fraction; Treg, Foxp3+ regulatory T cells.

( $P = .04$ ). These results highlight that peritumoral activated HSCs can aggravate chronic inflammation and fibrosis, which are suitable for tumor survival. Therefore, we attribute the prorecurrence power of peritumoral activated HSCs partly to their involvement in the inflammation response.

We also elucidated a positive relation of the density of peritumoral activated HSCs with that of M $\Phi$  or Tregs, which are confirmed predictors of poorer clinical outcomes, as shown in our study (Table 4) and other reports.<sup>2,5,38</sup> In addition, high densities of HSCs, M $\Phi$ , and Tregs are all related to aggressive clinicopathologic features, especially vascular invasion ( $P = .024$ ,  $P = .035$ , and  $P = .036$ , respectively, Table 5). Together with the facts that M $\Phi$  and Tregs are indispensable components of the sophisticated immunosuppressive network of HCC<sup>2,3,38</sup> and peritumoral activated HSCs are likely to cooperate with them to aggravate immunosuppression,<sup>11,13,39</sup> it is reasonable for us to suggest that peritumoral activated HSCs may also participate in the formation of the peritumoral immunosuppressive environment for the benefit of HCC recurrence.

Although many independent prognostic factors were found in the present study, it is still imperative to compare their predictive value. In our study, the predictive power of the density of peritumoral activated HSCs in combination with the *FAP* mRNA level was the best among all independent prognostic markers for HCC recurrence (area under the curve, 0.721, Table 6). Therefore, besides traditional prognostic factors, peritumoral activated HSCs are of clinical usefulness for predicting the postoperative recurrence of HCC.

We demonstrate that peritumoral activated HSCs are independent predictors for HCC recurrence and death, mainly via their proinflammatory and immunosuppressive activities. Our study implies that postoperative adjuvant therapies that target the soil, that is, the peritumoral liver tissues, to make it resistant to tumor growth are promising antirecurrence strategies. Obviously, interrupting or reversing the activation of peritumoral HSCs may be effective to reduce HCC recurrence and prolong survival.

*From the Liver Cancer Institute, Zhongshan Hospital and Shanghai Medical School of Fudan University, Key Laboratory for Carcinogenesis and Cancer Invasion, Chinese Ministry of Education, Shanghai, Peoples Republic of China.*

*Supported by grant 30700794 from the National Natural Science Foundation of China, Beijing; grant 107039 from the Chinese Ministry of Education, Beijing; and grant 2008ZX10208 from the National Key Sci-Tech Special Project of China, Beijing.*

*Address reprint requests to Dr Tang: Liver Cancer Institute and Zhongshan Hospital, Fudan University, 136 Yi Xue Yuan Rd, Shanghai 200032, P. R. China.*

*\*These authors contributed equally to this work.*

## References

- Parkin DM, Bray F, Ferlay J, et al. Global cancer statistics, 2002. *CA Cancer J Clin*. 2005;55:74-108.
- Gao Q, Qiu SJ, Fan J, et al. Intratumoral balance of regulatory and cytotoxic T cells is associated with prognosis of hepatocellular carcinoma after resection. *J Clin Oncol*. 2007;25:2586-2593.
- Zhu XD, Zhang JB, Zhuang PY, et al. High expression of macrophage colony-stimulating factor in peritumoral liver tissue is associated with poor survival after curative resection of hepatocellular carcinoma. *J Clin Oncol*. 2008;26:2707-2716.
- Sun HC, Zhang W, Qin LX, et al. Positive serum hepatitis B e antigen is associated with higher risk of early recurrence and poorer survival in patients after curative resection of hepatitis B-related hepatocellular carcinoma. *J Hepatol*. 2007;47:684-690.
- Budhu A, Forgues M, Ye QH, et al. Prediction of venous metastases, recurrence, and prognosis in hepatocellular carcinoma based on a unique immune response signature of the liver microenvironment. *Cancer Cell*. 2006;10:99-111.
- Yuki K, Hirohashi S, Sakamoto M, et al. Growth and spread of hepatocellular carcinoma: a review of 240 consecutive autopsy cases. *Cancer*. 1990;66:2174-2179.
- Kisseleva T, Brenner DA. Role of hepatic stellate cells in fibrogenesis and the reversal of fibrosis. *J Gastroenterol Hepatol*. 2007;22(suppl 1):S73-S78.
- Nakatani K, Seki S, Kawada N, et al. Expression of SPARC by activated hepatic stellate cells and its correlation with the stages of fibrogenesis in human chronic hepatitis. *Virchows Arch*. 2002;441:466-474.
- El-Karef A, Kaito M, Tanaka H, et al. Expression of large tenascin-C splice variants by hepatic stellate cells/myofibroblasts in chronic hepatitis C. *J Hepatol*. 2007;46:664-673.
- Levy MT, McCaughan GW, Marinos G, et al. Intrahepatic expression of the hepatic stellate cell marker fibroblast activation protein correlates with the degree of fibrosis in hepatitis C virus infection. *Liver*. 2002;22:93-101.
- Yin Z, Jiang G, Fung JJ, et al. ICAM-1 expressed on hepatic stellate cells plays an important role in immune regulation. *Microsurgery*. 2007;27:328-332.
- Friedman SL. Hepatic stellate cells: protean, multifunctional, and enigmatic cells of the liver. *Physiol Rev*. 2008;88:125-172.
- Chen CH, Kuo LM, Chang Y, et al. In vivo immune modulatory activity of hepatic stellate cells in mice. *Hepatology*. 2006;44:1171-1181.
- Novo E, Cannito S, Zamara E, et al. Proangiogenic cytokines as hypoxia-dependent factors stimulating migration of human hepatic stellate cells. *Am J Pathol*. 2007;170:1942-1953.
- Gulubova MV. Collagen type IV, laminin, alpha-smooth muscle actin (alphaSMA), alpha1 and alpha6 integrins expression in the liver with metastases from malignant gastrointestinal tumours. *Clin Exp Metastasis*. 2004;21:485-494.
- Olaso E, Santisteban A, Bidaurrezaga J, et al. Tumor-dependent activation of rodent hepatic stellate cells during experimental melanoma metastasis. *Hepatology*. 1997;26:634-642.
- Olaso E, Salado C, Egilegor E, et al. Proangiogenic role of tumor-activated hepatic stellate cells in experimental melanoma metastasis. *Hepatology*. 2003;37:674-685.
- Infante JR, Matsubayashi H, Sato N, et al. Peritumoral fibroblast SPARC expression and patient outcome with resectable pancreatic adenocarcinoma. *J Clin Oncol*. 2007;25:319-325.

19. Henry LR, Lee HO, Lee JS, et al. Clinical implications of fibroblast activation protein in patients with colon cancer. *Clin Cancer Res.* 2007;13:1736-1741.
20. Faouzi S, Lepreux S, Bedin C, et al. Activation of cultured rat hepatic stellate cells by tumoral hepatocytes. *Lab Invest.* 1999;79:485-493.
21. Mikula M, Proell V, Fischer AN, et al. Activated hepatic stellate cells induce tumor progression of neoplastic hepatocytes in a TGF-beta dependent fashion. *J Cell Physiol.* 2006;209:560-567.
22. Neaud V, Faouzi S, Guirouilh J, et al. Human hepatic myofibroblasts increase invasiveness of hepatocellular carcinoma cells: evidence for a role of hepatocyte growth factor. *Hepatology.* 1997;26:1458-1466.
23. Le Pabic H, Bonnier D, Wewer UM, et al. ADAM12 in human liver cancers: TGF-beta-regulated expression in stellate cells is associated with matrix remodeling. *Hepatology.* 2003;37:1056-1066.
24. Enzan H, Himeno H, Iwamura S, et al. Alpha-smooth muscle actin-positive perisinusoidal stromal cells in human hepatocellular carcinoma. *Hepatology.* 1994;19:895-903.
25. Varotti G, Ramacciato G, Ercolani G, et al. Comparison between the fifth and sixth editions of the AJCC/UICC TNM staging systems for hepatocellular carcinoma: multicentric study on 393 cirrhotic resected patients. *Eur J Surg Oncol.* 2005;31:760-767.
26. Edmondson HA, Steiner PE. Primary carcinoma of the liver: a study of 100 cases among 48,900 necropsies. *Cancer.* 1954;7:462-503.
27. Schepke M, Roth F, Fimmers R, et al. Comparison of MELD, Child-Pugh, and Emory model for the prediction of survival in patients undergoing transjugular intrahepatic portosystemic shunting. *Am J Gastroenterol.* 2003;98:1167-1174.
28. Marrero JA, Fontana RJ, Barrat A, et al. Prognosis of hepatocellular carcinoma: comparison of 7 staging systems in an American cohort. *Hepatology.* 2005;41:707-716.
29. Cai XY, Gao Q, Qiu SJ, et al. Dendritic cell infiltration and prognosis of human hepatocellular carcinoma. *J Cancer Res Clin Oncol.* 2006;132:293-301.
30. Cassiman D, Libbrecht L, Desmet V, et al. Hepatic stellate cell/myofibroblast subpopulations in fibrotic human and rat livers. *J Hepatol.* 2002;36:200-209.
31. Lissbrant IF, Stattin P, Wikstrom P, et al. Tumor associated macrophages in human prostate cancer: relation to clinicopathological variables and survival. *Int J Oncol.* 2000;17:445-451.
32. Gao Q, Wang XY, Fan J, et al. Selection of reference genes for real-time PCR in human hepatocellular carcinoma tissues. *J Cancer Res Clin Oncol.* 2008;134:979-986.
33. Livak KJ, Schmittgen TD. Analysis of relative gene expression data using real-time quantitative PCR and the 2(-Delta Delta C(T)) method. *Methods.* 2001;25:402-408.
34. Rajput AB, Turbin DA, Cheang MC, et al. Stromal mast cells in invasive breast cancer are a marker of favourable prognosis: a study of 4,444 cases. *Breast Cancer Res Treat.* 2008;107:249-257.
35. Poon RT-P, Fan ST, Ng IO, et al. Different risk factors and prognosis for early and late intrahepatic recurrence after resection of hepatocellular carcinoma. *Cancer.* 2000;89:500-507.
36. Iizuka N, Oka M, Yamada-Okabe H, et al. Oligonucleotide microarray for prediction of early intrahepatic recurrence of hepatocellular carcinoma after curative resection. *Lancet.* 2003;361:923-929.
37. Levy MT, McCaughan GW, Abbott CA, et al. Fibroblast activation protein: a cell surface dipeptidyl peptidase and gelatinase expressed by stellate cells at the tissue remodelling interface in human cirrhosis. *Hepatology.* 1999;29:1768-1778.
38. Mantovani A, Sozzani S, Locati M, et al. Macrophage polarization: tumor-associated macrophages as a paradigm for polarized M2 mononuclear phagocytes. *Trends Immunol.* 2002;23:549-555.
39. Marra F, Valente AJ, Pinzani M, et al. Cultured human liver fat-storing cells produce monocyte chemotactic protein-1: regulation by proinflammatory cytokines. *J Clin Invest.* 1993;92:1674-1680.

# First and Only FDA Cleared Digital Cytology System

**Genius™ Cervical AI**

**Genius™ Review Station**

**Genius™ Digital Imager**



## Empower Your Genius With Ours

**Make a Greater Impact on Cervical Cancer**  
with the Advanced Technology of the  
Genius™ Digital Diagnostics System



Click or Scan  
to discover more

ADS-04159-001 Rev 001 © 2024 Hologic, Inc. All rights reserved. Hologic, Genius, and associated logos are trademarks and/or registered trademarks of Hologic, Inc. and/or its subsidiaries in the United States and/or other countries. This information is intended for medical professionals in the U.S. and other markets and is not intended as a product solicitation or promotion where such activities are prohibited. Because Hologic materials are distributed through websites, podcasts and tradeshows, it is not always possible to control where such materials appear. For specific information on what products are available for sale in a particular country, please contact your Hologic representative or write to [diagnostic.solutions@hologic.com](mailto:diagnostic.solutions@hologic.com).

**genius™**  
DIGITAL DIAGNOSTICS